

NAG3-1274

FINAL  
IN-29-CR

34006

OCIT  
P. 25

Final Technical Report

To

The National Aeronautics and Space Administration

For the Grant on

"Chemical Vapor Deposition of High  $T_c$  Superconducting

Films in a Microgravity Environment"

June 1, 1991 to June 14, 1994

Prepared by

Moises Levy and Bimal K. Sarma

Physics Department and Laboratory for Surface Studies

University of Wisconsin-Milwaukee

Milwaukee, WI 53201

(NASA-CR-197527) CHEMICAL VAPOR  
DEPOSITION OF HIGH  $T_c$  (SUB  $c$ )  
SUPERCONDUCTING FILMS IN A  
MICROGRAVITY ENVIRONMENT Final  
Technical Report, 1 Jun. 1991 - 14  
Jun. 1994 (Wisconsin Univ.) 25 p

N95-16880

Unclass

G3/29 0034006

## **T A B L E   O F   C O N T E N T S**

### **A.    TECHNICAL REPORT**

1.    Introduction
2.    Formation and Characterization of the YBCO Thin Film

### **B.    PUBLICATIONS**

### **C.    PERSONNEL**

### **D.    REPRINTS**

Chemical Vapor Deposition of High  $T_c$  Superconducting Films  
in a Microgravity Environment

A. TECHNICAL REPORT

1. Introduction

Since the discovery of the YBaCuO bulk materials in 1987, Metalorganic Chemical Vapor Deposition (MOCVD) has been proposed for preparing HTSC high  $T_c$  films. This technique is now capable of producing high- $T_c$  superconducting thin films comparable in quality to those prepared by any other methods. The MOCVD technique has demonstrated its superior advantage in making large area high quality HTSC thin films and will play a major role in the advance of device applications of HTSC thin films.

The organometallic precursors used in the MOCVD preparation of HTSC oxide thin films are most frequently metal beta-diketonates. High  $T_c$  superconductors are multi-component oxides which require more than one component source, with each source, containing one kind of precursor. Because the volatility and stability of the precursors are strongly dependent on temperature, system pressure, and carrier gas flow rate, it has been difficult to control the gas phase composition, and hence film stoichiometry. In order circumvent these problems we have built and tested a single source MOCVD reactor in which a specially designed vaporizer was employed (Fig. 1). This vaporizer can be used to volatilize a stoichiometric mixture of diketonates of yttrium, barium and copper to produce a mixed vapor in a 1:2:3 ratio respectively of the organometallics. This is accomplished even though the three compounds have significantly different volatilities. We have developed a model which provides insight into the process of vaporizing mixed precursors to produce high quality thin films of  $Y_1Ba_2Cu_3O_7$ . It shows that under steady state conditions the mixed organometallic vapor must have a stoichiometric ratio of the individual organometallics identical to that in the solid mixture.

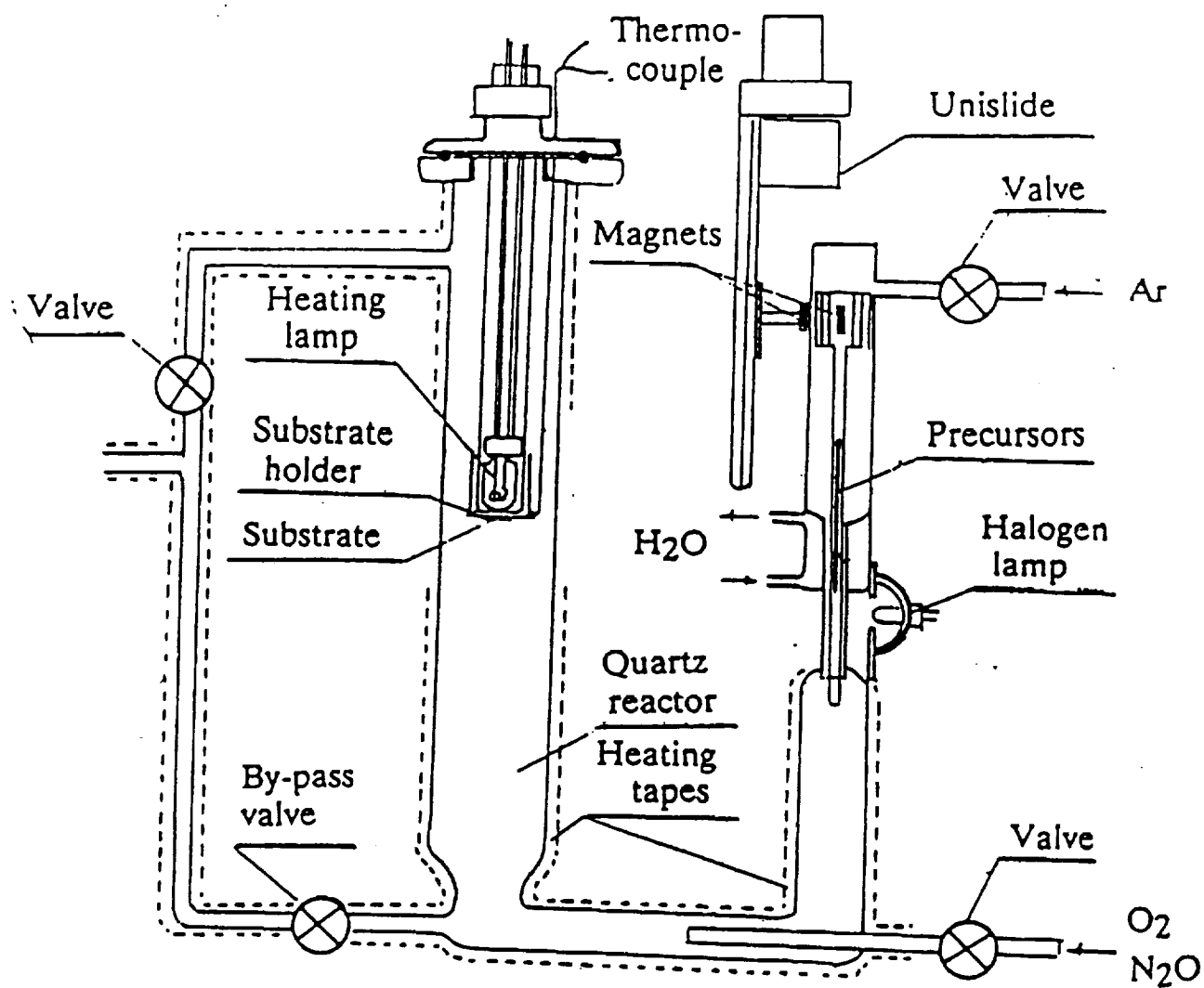


Fig. 1 Schematic diagram of the MOCVD system with single mixed precursors.

Fig. 2 is a schematic diagram of the vaporizer. Organometallic precursors are finely ground and mixed well, and then packed into a thin slotted glass tube. The tube slowly traverses an abrupt temperature gradient between the cooling jacket and the heating lamp which heats the mixed organometallic precursors to above 300°C, which is above the highest vaporization temperature of the three diketonates. Steady state vaporization of the powdered mixture occurs within the sharp temperature gradient and the vapors are transported to the substrate by a carrier gas which flows in the same direction as the movement of the slotted tube. This technique establishes a stream of mixed organometallic vapors with the desired composition.

We use an open channel carriage as the container for the mixed organometallics. The rectangular cross section carriage has an internal width,  $w$ , and height  $h$  as shown in Fig. 2. We assume that the mixed powder contains three compounds A, B and C in volume concentrations  $q_A$ ,  $q_B$ , and  $q_C$ , and that the surface vaporization rate of the individual compounds  $r_A$ ,  $r_B$ , and  $r_C$  are only a function of temperature. The vaporization rates may be given by the Arrhenius relation

$$r_i = K_i \exp \left( -\frac{\Delta H_i}{RT} \right)$$

where  $\Delta H_i$  is the heat of vaporization for species  $i$ ,  $R$  the gas constant, and  $K_i$  is the frequency factor. Fig. 3 shows the composition profile that may develop along the length of the melt of the precursors within the heating zone. As the melted wedge in Fig. 3a moves through the heating zone the configuration becomes more and more favorable for the vaporization of the least volatile compound because of the increase in the percentage of the melt's total surface area that it occupies. A desirable result of this processes is that the length ( $l_b$ ) for the complete vaporization of the least volatile component is shortened to  $l_b$  and the lengths for the more

volatile components ( $l_a$  and  $l_c$ ) become longer; to  $l_a$  and  $l_c$ , respectively. In Fig. 3, the evaporation length  $l_i$  is the length along the total length of the melt, within the heating zone, in which component  $i$  is present, and  $q_i$  is the component concentration. The capital subscripts refer to evaporation when only a single precursor is loaded into the open channel carriage. The quantity of precursor  $i$  vaporized per unit time at position  $x$  along the length is

$$r_i w dl$$

The net quantity of precursor  $i$  entering position  $x$  is

$$wy(x) v q_i(x) - wy(x + \Delta x) v q_i(x + \Delta x)$$

In steady state, these two quantities should be equal and therefore we obtain

$$r_i = v \frac{y(x) dq_i(x) + q_i(x) dy}{dl}$$

Integration over length of this rate will yield the total vaporization rate in the heating zone

$$R_i = \int r_i w dl = -wv \int_{l_0}^{l_i} d(yq_i) = wv[(yq_i) l_0 - (yq_i) l_i] = whvq_i$$

These equations give two important properties of the vaporization: the ratio of the three compounds in the gas phase, and hence the film's elemental composition, is the same as that in the initial mixture, assuming the film composition is proportional to the gas phase (This is the mass continuity requirement.); and, the mass flow rate of each component is determined by the cross sectional area and the velocity of the carriage.

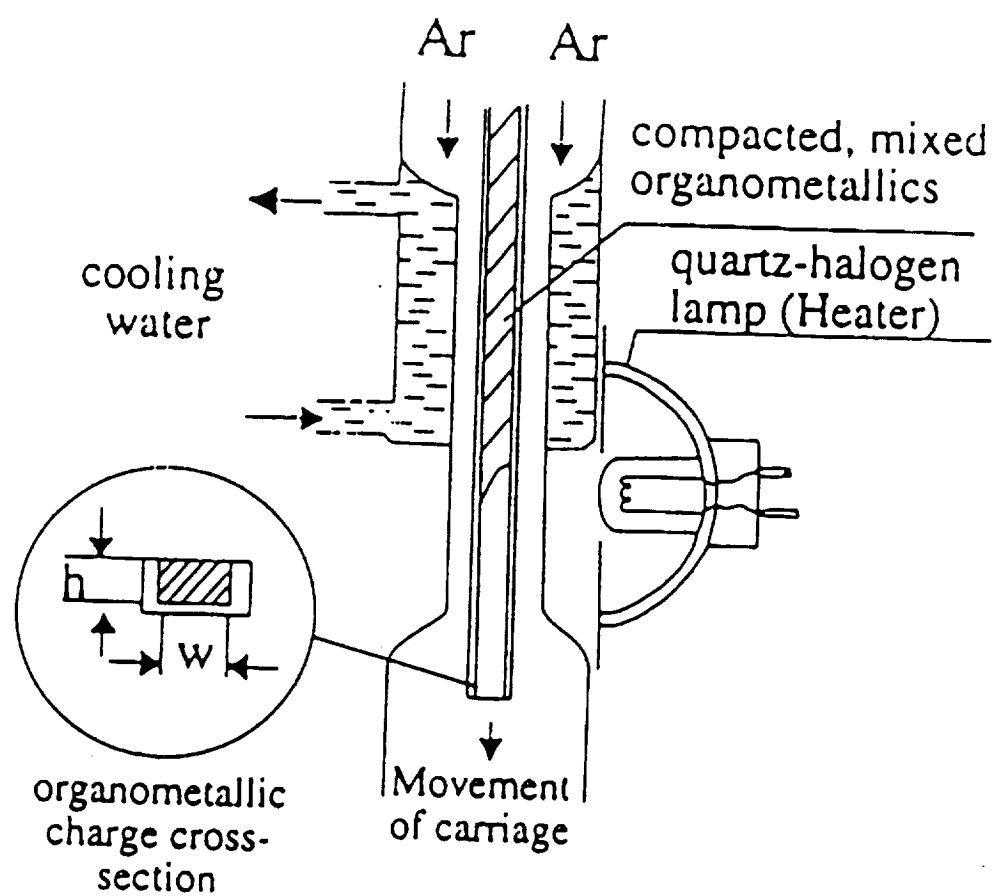


Fig. 2 The mixed organometallic precursors vaporizer.

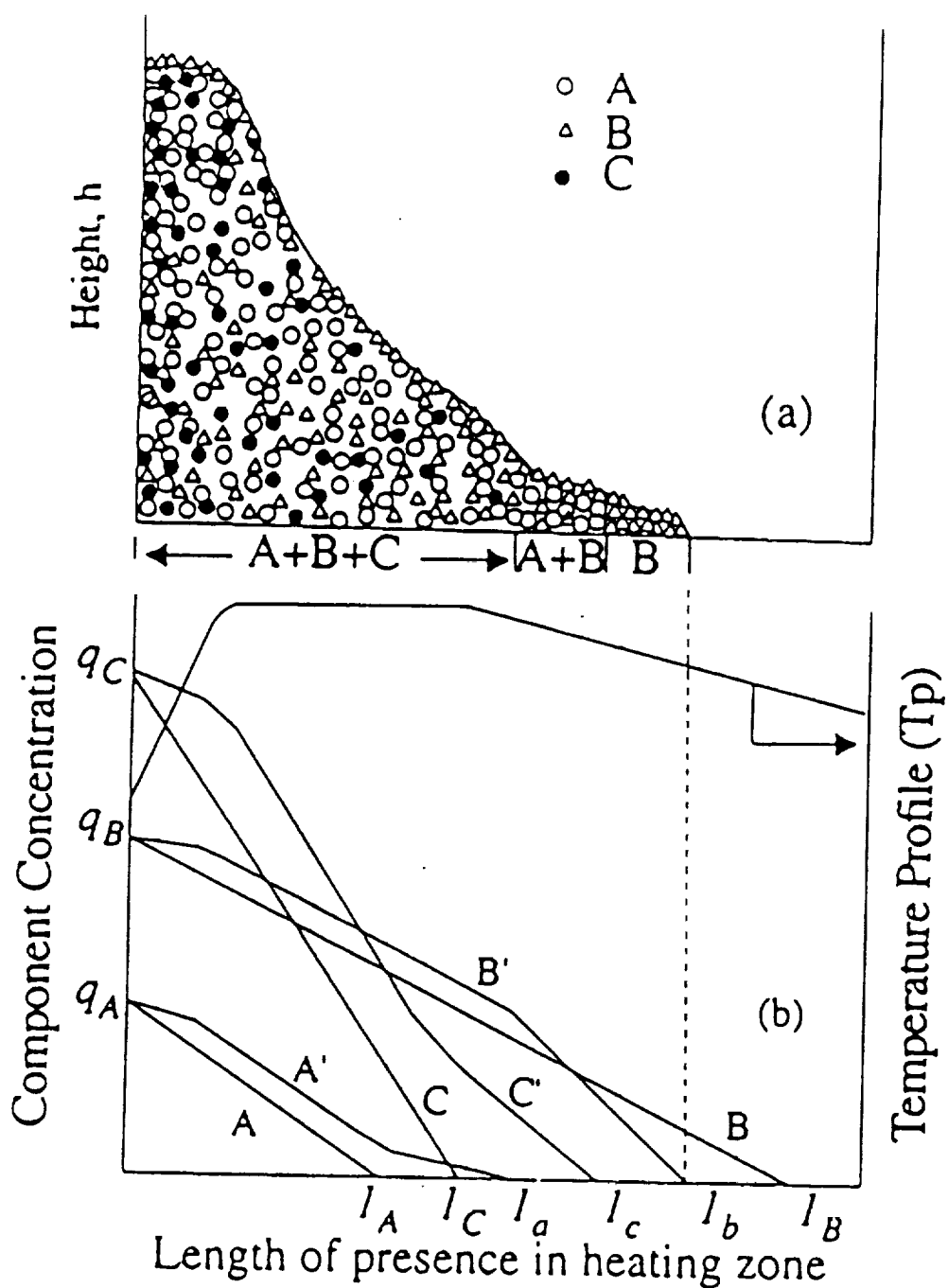


Fig. 3 Conditions with the heating zone (a) Profile of mixed organometallic wedge, showing the microstructure and nonuniform vaporization surface. (b) Revised component concentrations and temperature profile along heating zone length.



## 2. Formation and Characterization of the YBCO Thin Films

After successfully producing numerous films of superconducting  $Y_1Ba_2Cu_3O_7$  on MgO substrates and yttrium stabilized zirconia YSZ substrates, a set of experiments were performed to try to optimize the growth conditions of YBCO superconducting films on 13 mm diameter YSZ substrates. In order to do this, the substrate temperature ( $T_s$ ), carrier gas (Ar), oxygen ( $O_2$ ) flow rate and vapor pressure ( $P$ ) of the reactor were changed and all the other conditions were held constant during the growth process. Six different samples were made under the conditions shown in Table 1. The glass precursor source was made by compacting a mixture of  $Y(thd)_3$ ,  $Ba(thd)_2$  and  $Cu(thd)_2$  in the ratio  $Y:Ba:Cu = 1:2:3$  into a glass tube in a dry box.

Table 1. Conditions for growing samples No. 1 to 6

Sample	$T_s(^{\circ}C)$	$P(Torr)$	$O_2(sccm)$	$Ar(sccm)$
No.1	850	6	300	288
No.2	820	6	300	288
No.3	820	3	100	143
No.4	800	3	100	143
No.5	775	3	100	143
No.6	750	3	100	143

X-ray diffraction XRD patterns of samples 1-6 are shown in Figs. 4 a-f respectively.

Fig. 4b for sample 2 shows a perfectly c-axis (001) oriented 123 phase film. Fig. 4a for

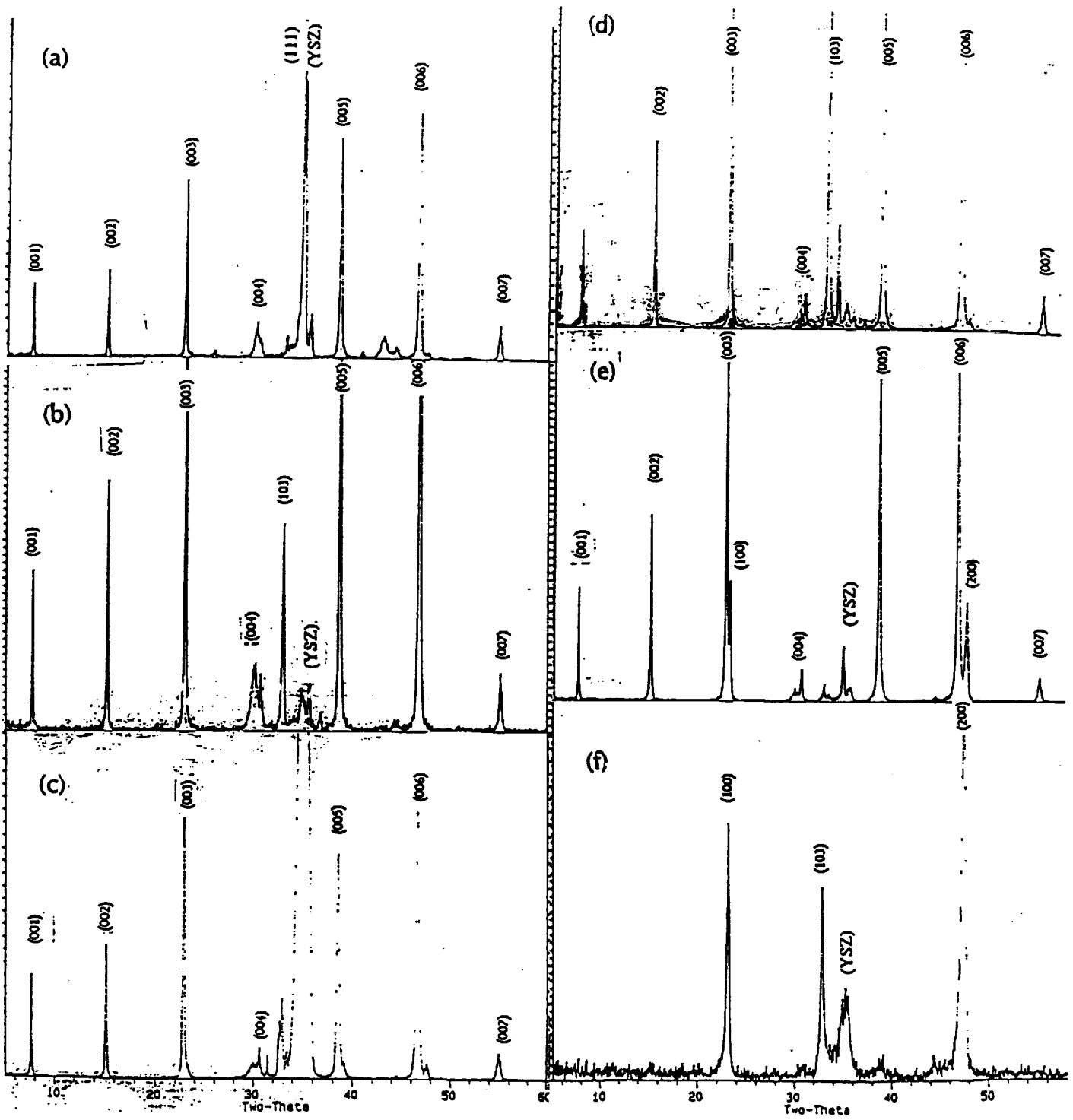


Fig. 4 X-ray diffraction patterns of samples No. 1 to No. 6.

sample 1 shows that this film has (111) oriented 123 phase mixed with the (001) orientation. We find that these results are consistent with resistance versus temperature R-T measurements, which will be discussed later. Samples 3-6 were grown under the same conditions as for samples 1 and 2 except for the substrate temperature  $T_s$ . However their XRD patterns are very different. For samples 3 and 4 where  $T_s \geq 800^\circ\text{C}$ , the XRD's show almost perfect (001) 123 single phase. For  $T_s$  at  $775^\circ\text{C}$ , the (100) oriented 123 phase began to appear and was mixed in with the (001) phase as shown in Fig. 4e. Finally, when  $T_s$  was  $750^\circ\text{C}$  the film phase was a perfectly oriented a-axis (100) 123 film (Fig. 4f). These results show that a-axis oriented films were grown on YSZ (100) substrates at lower substrate temperatures. The c-axis (001) phase and a-axis (100) phase competed with each other at substrate temperatures  $T_s$  ranging from 750 to  $820^\circ\text{C}$ . These results emphasize that the competition is so strongly dependent on substrate temperature that a  $T_s$  change of just  $50^\circ\text{C}$  will change the 123 phase from c-axis to a-axis. This means that the key to controlling the c-axis or a-axis 123 phase growth is controlling the substrate temperature, at least at the vapor pressures used in our reactor.

The temperature dependence of the resistances of samples 1- 5 is shown in Fig. 5. The  $T_{co}$ 's ( $R=0$ ) of samples 1-5 were  $<70$  K, 89.3 K, 80 K, 79 K, and 86 K, respectively. The temperature dependence of the resistance of sample 6 showed semiconducting behavior, increasing with decreasing temperature down to 70 K. It appears that the lower the partial pressure of  $\text{O}_2$ ,  $P(\text{O}_2)$ , the lower the optimum substrate temperature. The substrate temperature and reactor pressure for making sample 2 in our reactor produced the highest  $T_c$ , around 90 K, and the narrowest transition width,  $<1$  K of all our films. In our MOCVD system the optimum conditions are produced by an interplay between the partial pressure in the reactor and the substrate temperature. At different pressures, the optimum  $T_s$  for perfect (001) 123 phase growth is different, the higher the pressure, the higher the optimum  $T_s$ .

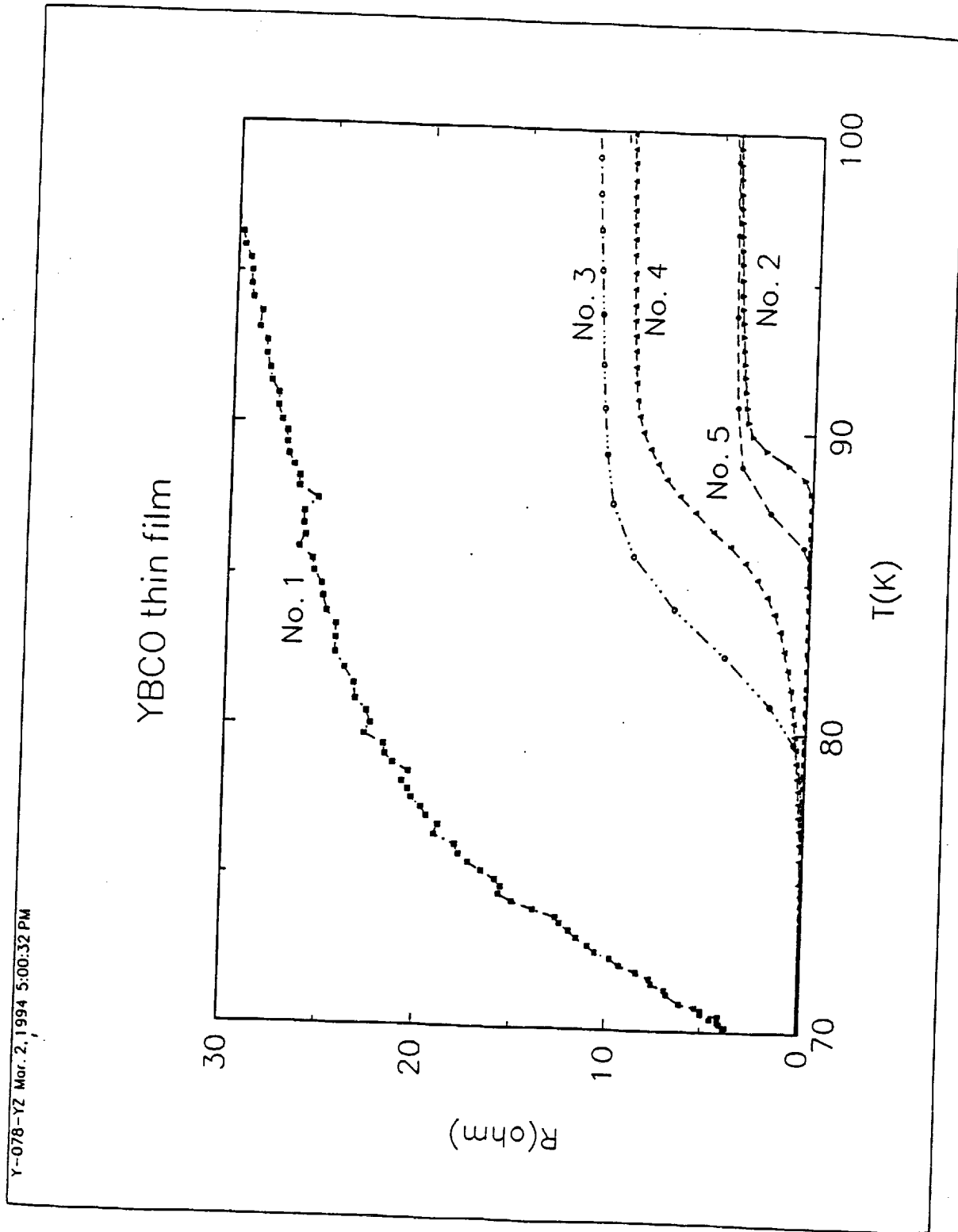


Fig. 5 Temperature dependence of resistivity for samples No. 1 to 5.

For quantitatively measuring the homogeneity of the film surface, a line analysis of the 2D image of sample 2 by Atomic Force Microscopy AFM and surface resistance by a four probe method were used. AFM data of the images of 8 different locations along a diameter on the surface of sample 2 were analyzed. The average  $R_{rms}$  (the root-mean-square roughness) and  $R_{ave}$  (the average roughness) are shown in Table 2 and in Fig. 6. The edge of the surface of this sample was rougher than the center, as seen in Fig. 6.

Table 2. Average  $R_{rms}$  (Å) and  $R_{ave}$  (Å) for 8 points(Pts) of the surface of the sample No.2

Pts	1	2	3	4	5	6	7	8
$R_{rms}$	1156.4	666.6	534.0	223.0	651.2	580.24	412.0	968.6
$R_{ave}$	757.2	400.6	341.0	161.4	380.6	276.0	266.6	652.4

The temperature dependence of the resistance at 5 different points along a diameter of the surface of sample 2 was measured by a four probe AC resistance bridge. The results are shown in Fig. 7. The  $T_{co}$ 's at the different points are 88.79 K, 89.19 K, 89.12 K, 88.95 K and 89.03 K, respectively. The average  $T_{co}$  is 89.02 K and the maximum deviation is  $\pm 0.23$  K.

The resistance at 12 different points along a diameter of sample 2 were measured by the four probe method. In this measurement, a small current  $I$  from a constant-current source is passed through the outer two probes and the voltage  $V$  is measured between the inner two probes (distance  $s$ ). For a thin film (diameter  $d$ ) with thickness  $w$  much smaller than either  $s$  or  $d$ , the sheet resistance  $R_s$  is given by

$$R_s = (V/I) \cdot C \quad \Omega/\text{square}$$

where  $R_m = V/I$  is the measured resistance, and the  $C$ 's are a geometrical correction factor.

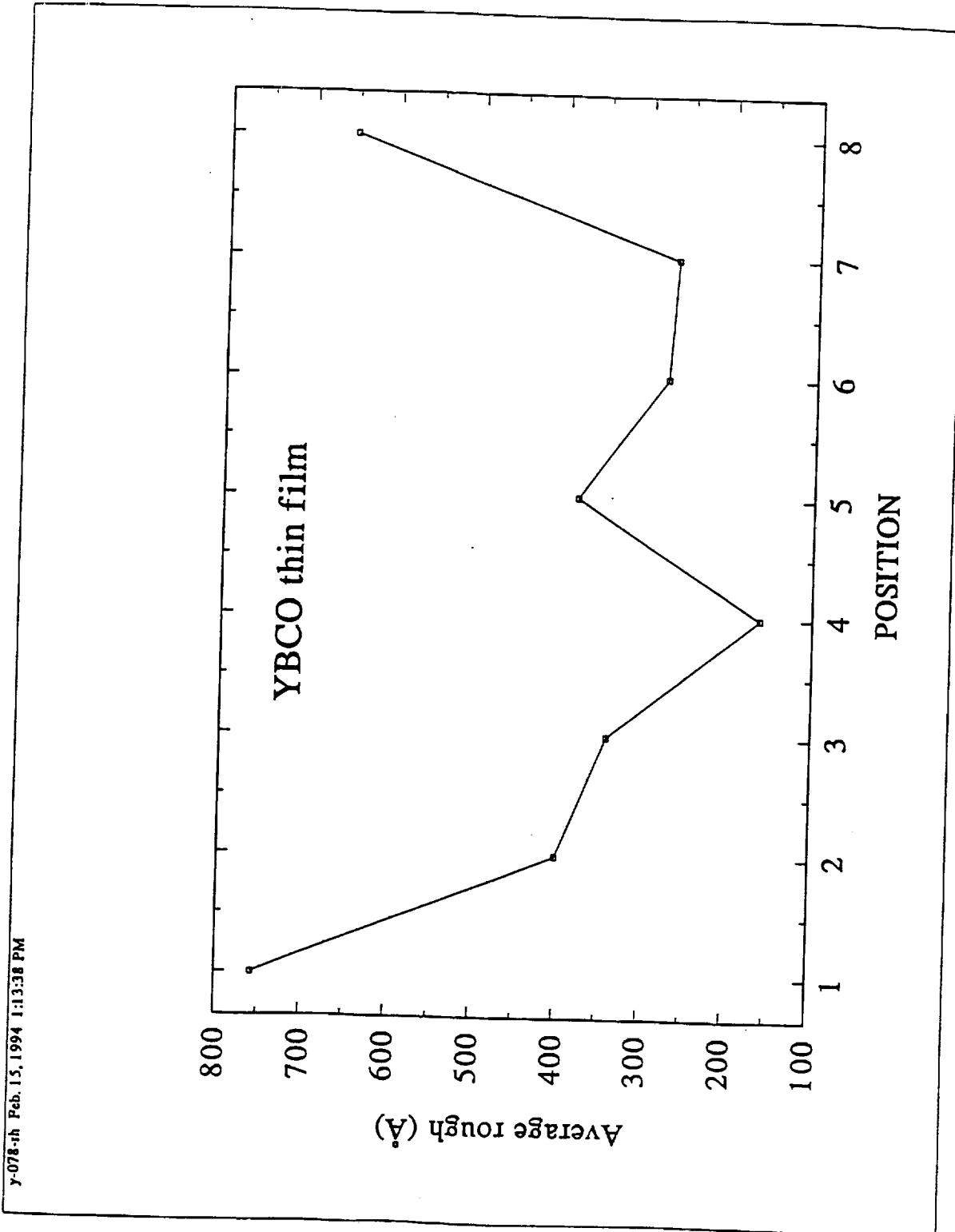


Fig. 6 The roughness of the surface of sample No. 2.

## YBCO Thin Film

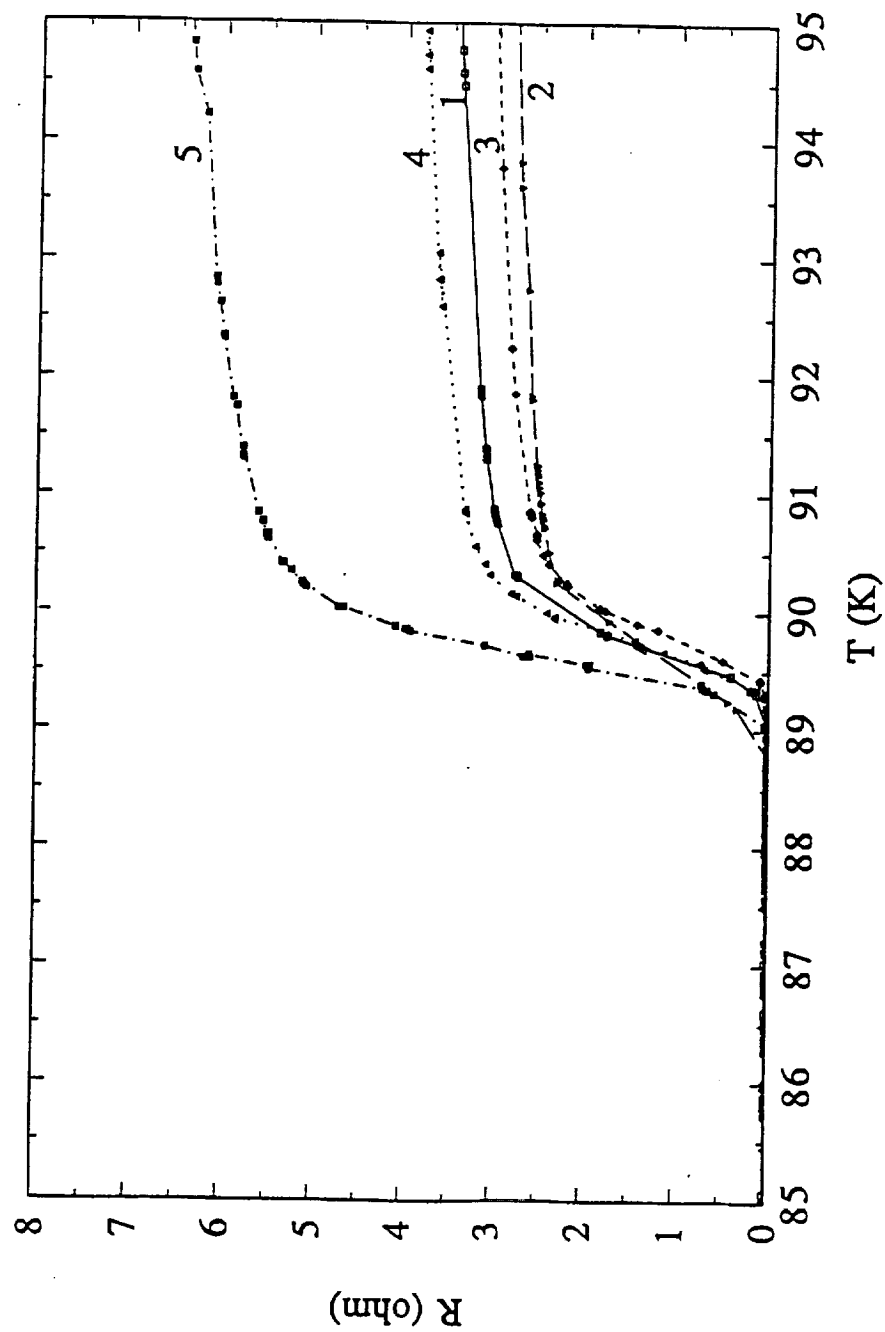


Fig. 7 The temperature dependence of resistances at 5 points along a diameter of the surface of sample No. 2.

The calculated  $C$ 's at the 12 points of the surface where the resistances were measured are given in Table 3. The  $R_s$  and  $R_m$  are also given in Table 3 and plotted in Fig. 8. The root-mean-square  $R_m$  is 3.2 and the root-mean-square  $R_s$  is 5.02 calculated from the data of the Table 3. The roughness at the edge of the film is larger than at the center, but does not appear to correlate with  $T_{co}$ .

Table 3. Values of  $C$ ,  $R_m$  and  $R_s$  at 12 points along a diameter of the surface of sample No.2

Point	$C$	$R_m$	$R_s$
1	2.52	16.39	41.30
2	3.588	12.52	44.92
3	4.007	9.44	37.83
4	4.171	8.85	36.91
5	4.243	8.13	34.50
6	4.272	9.08	38.89
7	4.272	8.69	37.12
8	4.243	9.87	41.88
9	4.171	8.16	34.04
10	4.007	11.81	47.32
11	3.588	13.91	49.91
12	2.52	17.22	43.39



# YBCO thin film

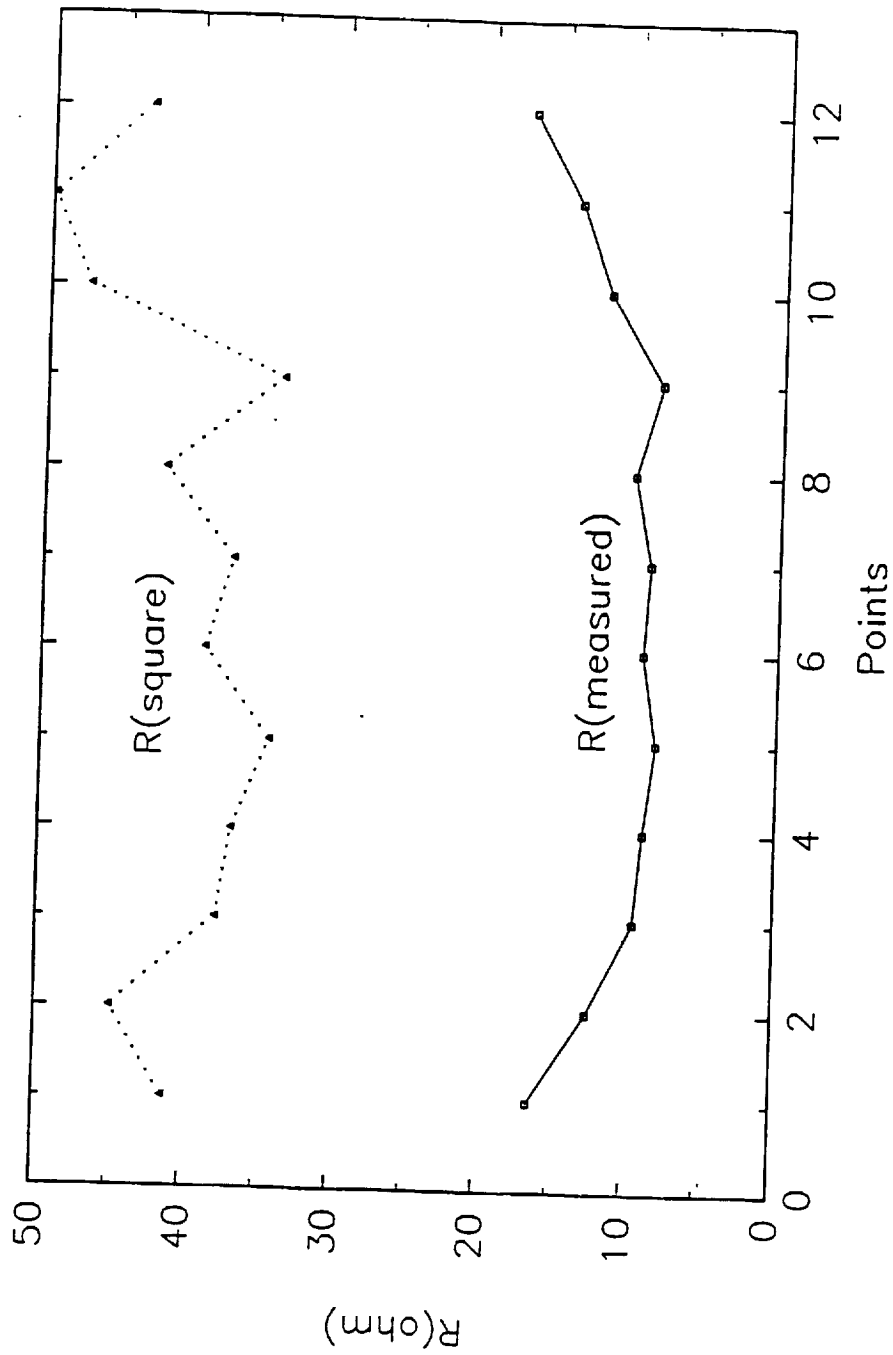


Fig. 8 Plot of the resistances at 12 points along the diameter of the surface of sample No. 2.

High quality YBCO thin films have been deposited. These films have good superconducting properties including high critical current densities,  $J_c$ . The vortex pinning centers responsible for the high  $J_c$ 's are believed to be related to the crystal defects in the films, since bulk YBCO single crystals have much lower  $J_c$ 's, but the defects responsible for the high  $J_c$ 's in films have not been identified. Thus studies of the initial growth mechanisms and of the formation and evolution of the dislocations and other defects could provide useful information, leading to the identification of the vortex pinning centers. A study of the initial growth mechanism may ultimately enable us to either eliminate or introduce the relevant defects in a controlled way for different applications. Fig. 9a shows the YBCO 123 phase spiral growth structure observed by AFM. From a line analysis, in Fig. 9b we can see that the step for the spiral is about 12 Å. This structure was obtained on a thick film (5000 Å). Further study of the initial growth process will help to determine the spiral growth model, which could be island formation (Volmer-Weber model), or layer-by-layer, or layer-by-layer followed by island growth (Stranski-Krastanov model).

The vaporization of the precursors is affected by gravity. As we discussed before, in order to maintain stoichiometry after the gas evolves from the heating zone, it is imperative that all the premixed powders entering the heating zone are vaporized by the time they tranverse the heating zone. During travel through the heating zone the precursor melt develops an asymmetric curved surface. The shape and the length of the melt wedge are functions of the feed rate of the precursors. Along the length, the leading section will be rich in the least volatile (high vaporization temperature) component such as  $\text{Ba}(\text{thd})_2$ . Since the tube is moving vertically, there is a tendency for the liquid phase to flow downwards through the heating zone before it is fully vaporized. When this happens, the resulting gas phase is not stoichiometric and therefore the deposited film cannot be of the correct composition. To solve this problem, we are proposing

Sep 14 94 s7  
Y-110 Mgo new  
825 C O2 300 Ar 200

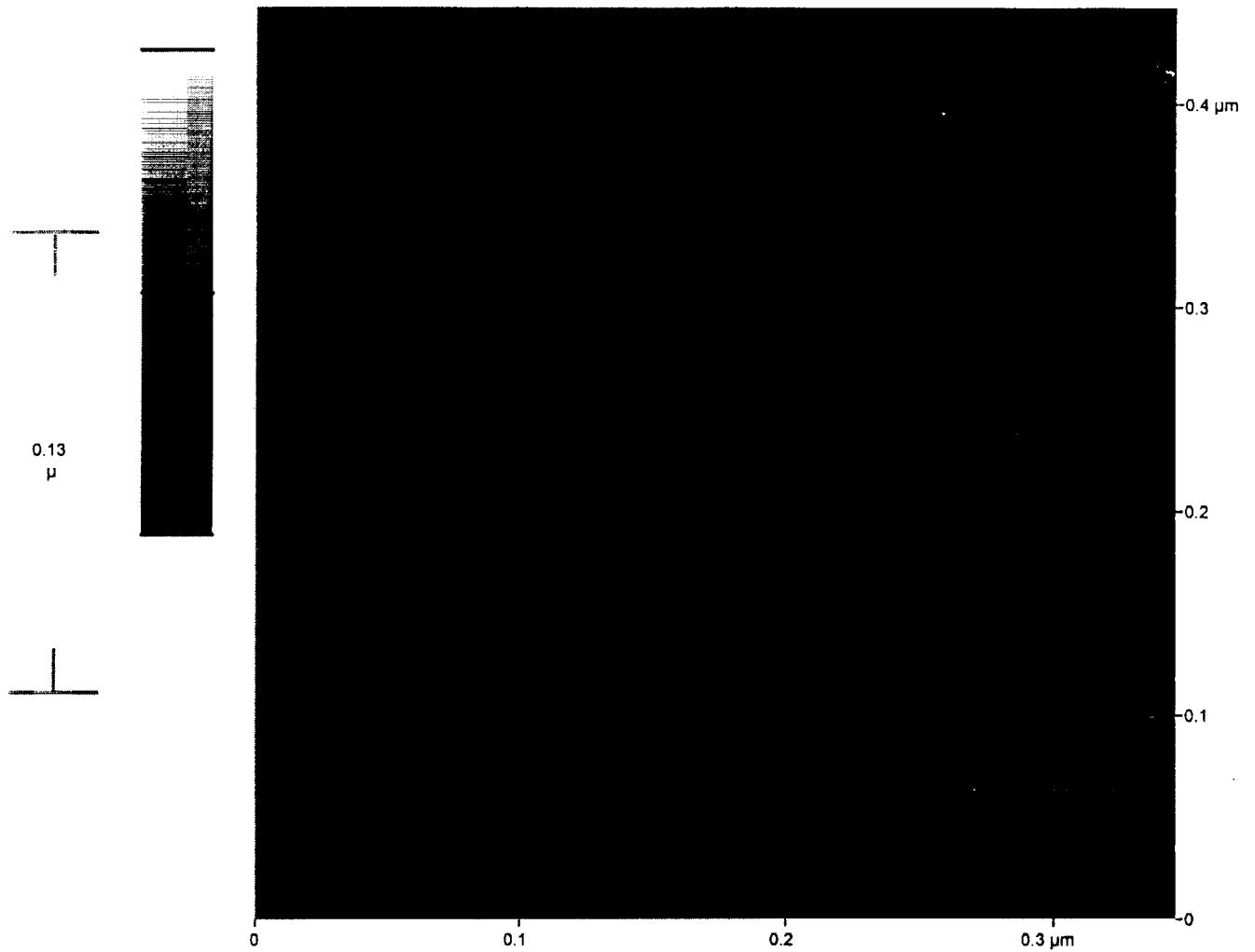
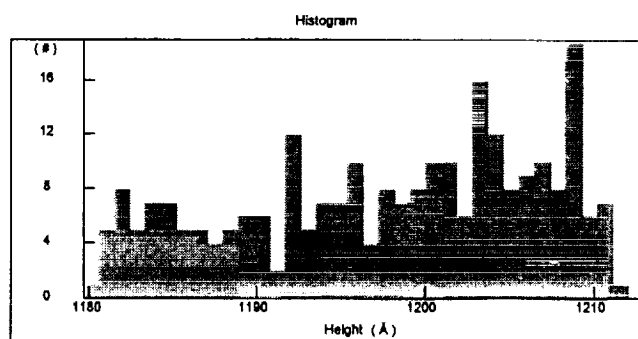
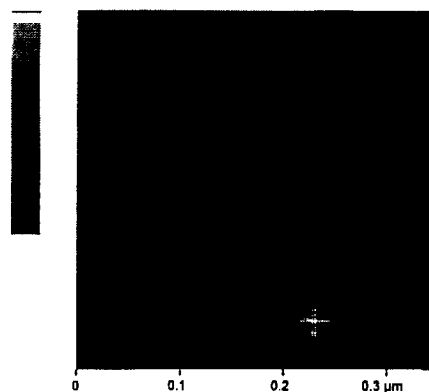


Fig. 9a AFM image showing the spiral growth of YBCO c-axis 123 phase.

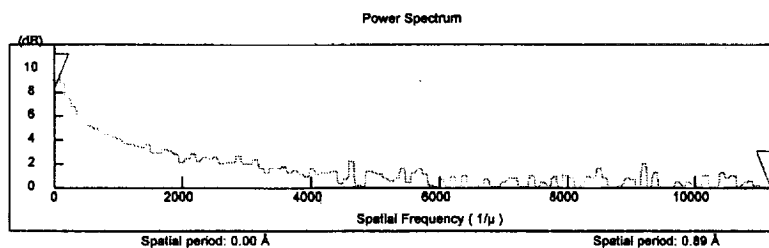
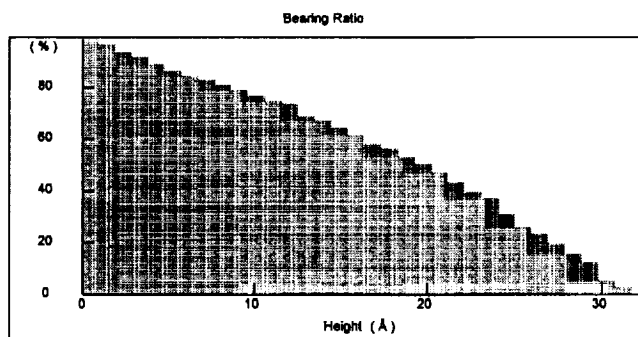
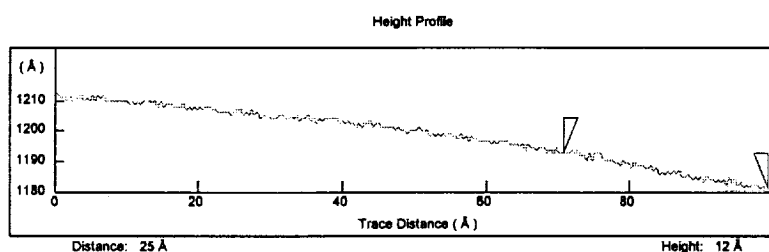
12/20/94 11:23

## LINE ANALYSIS

Sep 14 94 s7  
Y-110 Mgo new  
825 C O2 300 Ar 200



12/20/94 11:34



Trace Statistics :  
Height : 12 Å  
Spacing : 25 Å  
Angle : 25.1°  
Distance : 27 Å  
Arc length : 323 Å

Peak to valley : 33 Å  
Median height : 1200 Å  
Mean height : 1198 Å  
Rms rough : 9.1 Å  
Ave rough : 7.8 Å

Fig. 9b AFM image line-scan profile showing that a step for this spiral is about 12 Å which is equal to the c-length of the 123 phase cell.

to turn the reactor so that the precursor tube travels through the heating zone horizontally. A microgravity environment would be important in assuring that the mixed organometallic precursors would be completely vaporized in the heating zone.

## B. PUBLICATIONS

During this research project four papers have been published or prepared for publication which describe the MOCVD reactor operation and the films that have been deposited in this reactor. The abstracts of each paper follows the respective title. Complete copies of the four papers are included in the appendix.

1. "Model for the Vaporization of Mixed Organometallic Compounds in the Metalorganic Chemical Vapor Deposition of High Temperature Superconducting Compounds," Guangyao Meng, Gang Zhou, Roger Schneider, Bimal K. Sarma, and Moises Levy, Appl. Phys. Lett. 63, 1981-1983 (1993).

A model of the vaporization and mass transport of mixed organometallics from a single source for thin film metalorganic chemical vapor deposition is presented. A stoichiometric gas phase can be obtained from a mixture of the organometallics in the desired mole ratios, in spite of differences in the volatilities of the individual compounds. Proper film composition and growth rates are obtained by controlling the velocity of a carriage containing the organometallics through the heating zone of a vaporizer.

2. "Formation and Characterization of  $\text{YBa}_2\text{Cu}_3\text{O}_{7-\delta}$  high  $T_c$  Thin Films by MOCVD With Single Mixed Precursor," Guangyao Meng, Gang Zhou, Roger Schneider, Bimal K. Sarma, and Moises Levy, Physica C 214, 297-306 (1993).

In view of the promising role of the MOCVD technique in the advance of YBCO high- $T_c$  superconducting thin films grown for device applications, a simplified chemical vapor deposition system with a single mixed organometallic precursor was built and tested. Single phase  $\text{YBa}_2\text{Cu}_3\text{O}_{7-\delta}$  films with  $T_c$  values around 90 K were readily obtained on (100) YSZ and (100) MgO substrates with a normal precursor mass transport. Investigations indicate that, in addition to the gas phase stoichiometry as a major factor,

the phase composition and crystallite orientations of the YBCO films were considerably affected by the oxidation agent (partial pressure and concentration) as well as the substrate temperature. The films could be either highly oriented (001) or (100) and/or (110) orientation dominated. A single phase  $\text{Y}_2\text{Cu}_2\text{O}_5$  film with (002) orientation was obtained from a Ba deficient gas phase. The variation in superconducting behavior of the YBCO thin films deposited under different conditions was not only related to these phase but also to the growth orientation. The film uniformity and flatness are examined and discussed in terms of the gas flow pattern in the reactor.

3. "Vaporization of Mixed Precursors in Chemical Vapor Deposition of YBCO Films," Guangyao Meng, Gang Zhou, Roger Schneider, Bimal K. Sarma, and Moises Levy, *Journal of Superconductivity* **7**, 234-237 (1994).

Single phase  $\text{YBa}_2\text{Cu}_3\text{O}_{7-\delta}$  thin films with  $T_c$  values around 90 K are readily obtained by using a single source chemical vapor deposition technique with a normal precursor mass transport. The quality of the films is controlled by adjusting the carrier gas flow rate and the precursor feed rate.

4. "Studies of YBCO Thin Films on YSZ substrates by Single Source MOCVD," Gang Zhou, T. Deng, Jeffrey Feller, Roger L. Schneider, Bimal K. Sarma, and Moises Levy (to be submitted to *Physica C*).

YBCO superconducting films were prepared on YSZ(001) crystal substrates by a single source MOCVD using a mixture of powders of  $\text{Y}(\text{thd})_3$ ,  $\text{Ba}(\text{thd})_2$  and  $\text{Cu}(\text{thd})_2$ . A single crystal film, with  $T_{c0}$  89 K, was made under optimum conditions. The film homogeneity was determined by resistance and  $T_{c0}$  measurements at several points of the surface along a diagonal of the film. The change of resistance was less than 15% at room temperature and the change of  $T_{c0}$  was less than 0.3% of the average  $T_{c0}$ . The

roughness of the film was higher at the edge than at the center, but did not appear to affect its superconducting properties. C-axis and a-axis YBCO phase compete each other in the substrate temperature range between 750 and 820 C. The 3D morphology of films having different  $T_{c0}$ 's was studied with an Atomic Force Microscope. It was found that the shape and orientation of the grains composing the films were very closely related to the superconducting properties of the films.



### C. PERSONNEL

In addition to the principal investigator Moises Levy and the co-investigator Bimal K. Sarma the following personnel worked on this research project.

Assoc. Prof. Guangyao Meng	Visiting Scholar (11 months) from the Department of Material Science and Engineering, University of Science and Technology of China, Hefei, 230026, China
Assoc. Prof. Ting Zhang Deng	Visiting Scholar (2 months) Institute of Physics, Chinese Academy of Sciences, Beijing, China
Dr. Roger L. Schneider	(2 months salaried, the rest of the time free on an as needed basis) Whitefish Bay, Wisconsin
Mr. Gang Zhou	Graduate Research Assistant (Three and a half years) It is expected that Mr. Zhou will receive his Ph.D. in 1995.